

## Spin-polarized photoelectron diffraction using circularly polarized x rays

G. D. Waddill and J. G. Tobin

*Chemistry and Materials Science Department, Lawrence Livermore National Laboratory,  
P.O. Box 808, L-357, Livermore, California 94550*

X. Guo and S. Y. Tong

*Laboratory for Surface Studies and Department of Physics, University of Wisconsin–Milwaukee, Milwaukee, Wisconsin 53201*

(Received 17 May 1994)

The observation of spin-dependent photoelectron diffraction using circularly polarized x rays is reported for Fe films on Cu(001). Circularly polarized x rays produce spin-polarized photoelectrons from the Fe  $2p$  doublet, and intensity asymmetries in the  $2p_{3/2}$  level are observed. Fully spin-specific multiple-scattering calculations reproduce the experimentally determined energy and angular dependences. An analytical procedure is introduced which removes exchange shift contributions to the Fe  $2p$  asymmetry, and focuses instead upon intensity variations due to spin-dependent diffraction.

Ascertaining the nanoscale structure-property relationships of a magnetic surface, ultrathin film, or interface remains a formidable but potentially extraordinarily rewarding task. For example, as studies of giant magnetoresistive<sup>1</sup> and spin valve<sup>2</sup> systems have progressed, it has become clear that spin-specific interfacial scattering is a critical but poorly understood event. To properly address such problems, a probe which combines elemental specificity with a sensitivity to local order, both geometric and magnetic, is essential. Spin-polarized photoelectron diffraction (SPPD) is potentially an ideal candidate for studying nanoscale magnetic systems, with the above attributes plus the promise of an ultimate extension to element- and spin-specific imaging.<sup>3</sup> However, while the potential for SPPD is very high, particularly with the advent of third generation synchrotron-radiation facilities such as the Advanced Light Source, until now a definitive demonstration has been lacking. This is primarily because of the relatively inefficient nature of spin detectors and the relatively weak nature of magnetic scattering effects. Here we present a prototype study using magnetic x-ray circular dichroism, to permit a direct and unambiguous control of electron polarization without the necessity of the low-efficiency spin detectors. This is coupled with a fully spin-specific, multiple-scattering computational analysis. While we remained hampered by the limitations of existing sources of circularly polarized x rays and hence are constrained in terms of signal to noise, this is a definitive demonstration of SPPD and consequently permits us to project, via our spin-specific, multiple-scattering analysis, the direction of future work at third generation sources.

To provide a stringent test of SPPD, we chose to study Fe/Cu(001). This model system exhibits the perpendicular magnetization<sup>4</sup> that may be used in higher density magnetic recording media. Additionally, Fe/Cu(001) has been highly studied and the subject of considerable interest:<sup>5–10</sup> in fact, we reproduced the forward focusing photoelectron diffraction (PD) results of Chambers, Wagener, and Weaver<sup>5</sup> as an *in situ* cross check of alignment. Fe/Cu(001) at low temperatures and low coverages is an irregular fcc structure, thus exhibiting the template effects so crucial to manipulation of ultrathin prop-

erties plus providing a classical test of the sensitivity of photoelectron diffraction to local order.

In some respects, this SPPD investigation is an independent verification and extension of the pioneering studies of Schütz *et al.*,<sup>11</sup> who used spin-polarized extended x-ray absorption fine structure (EXAFS) to probe bulk magnetic systems. Consistent with nonspin PD and EXAFS studies, the SPPD shows a larger effect: the SPPD oscillations are on the order of 2%, while the Gd metal SPEXAFS oscillations are  $\leq \frac{1}{3}\%$ . Additionally, SPPD has the advantage of both energy and angular variations, which is essential to the extension to photoelectron diffraction imaging.<sup>3</sup> Both this work and the ground-breaking studies of Schütz *et al.*<sup>11</sup> are predicated upon control of spin polarization of ejected electrons via excitation with circularly polarized x rays. In a simplistic picture,  $2p$  photoemission total cross sections from ferromagnetic materials will exhibit a polarized distribution of 62.5% (37.5%) minority spin electrons from the  $2p_{3/2}$  and 25% (75%) minority spin electrons from the  $2p_{1/2}$ , when excited with right (left) circularly polarized radiation that is collinear with the magnetic axis of the sample. These adjustably spin-polarized electrons can then scatter off of nearby neighbors, producing a sensitivity to both local geometric and magnetic ordering. (Although we have chosen to use a ferromagnetic system as a test case, these same selection rules will apply in general, e.g., to paramagnetic and antiferromagnetic ordering, and the multiple-scattering analysis should be sensitive to differences in the local order of each structure.) To avoid extraneous effects and to allow internal cross checking of data, measurements were performed only in mirror planes, where only the relative alignment of the photon helicity and magnetization is crucial. Thus reversing the absolute value of these quantities, while maintaining the same relative spin orientation, serves as a convenient but absolutely essential consistency test to determine if the observed asymmetry is due to spin-dependent diffraction. It is the absence of such polarization control or electron-spin detection, plus the ill-defined nature of the intrinsic  $3s$  polarization, that has hampered previous attempts at SPPD using the  $3s$  level of  $3d$  transition metals.<sup>12–14</sup>

In this paper, we present experimental results for Fe

films on Cu(001) which demonstrate the spin-dependent photoelectron diffraction using circularly polarized x rays. Results for scattering along two high-symmetry directions demonstrate strong angular effects in the spin-dependent scattering, and we make an observation of spin-specific, energy-dependent photoelectron diffraction. Comparison of experimental results with fully spin-polarized multiple-scattering calculations demonstrates good agreement. This is a comparison between experiment and theory for spin-dependent scanned-energy photoelectron diffraction. To facilitate comparison, we introduce an analytical approach to dichroism asymmetry which removes the peak shift due to the exchange interaction in order to isolate the spin-dependent *intensity variations* due to diffraction. From this, we have obtained a detailed and unambiguous structural determination using SPPD. Finally, calculations with internally spin-polarized photoelectrons combined with external spin detection suggest that this will be a powerful technique for studying magnetic materials in the future.

The experiments were performed at the Stanford Synchrotron Radiation Laboratory using a spherical grating monochromator capable of delivering  $\sim 90\%$  circularly polarized radiation.<sup>15</sup> Four monolayer (ML) Fe films were grown on a Cu(001) substrate held at  $\sim 150$  K. This results in relatively poorly ordered metastable fcc Fe overlayers as evidenced by the diffuse  $p(1 \times 1)$  low-energy electron-diffraction (LEED) pattern observed for these films. These films have a magnetic easy axis along the sample normal,<sup>8,9</sup> and were magnetized *in situ* with an electromagnet coil. All measurements were made in remanence. The Fe  $2p$  spectra were collected with an angle-resolving hemispherical analyzer with angular acceptance of  $\pm 3^\circ$ . The magnetic axis dictated that the photoelectron polarization is maximized for photons incident along the sample normal. The analyzer position was adjusted to the desired electron emission angle. When the scattering plane contained the sample normal and the (110) azimuth, the electron emission was along the [111] direction. For the (100) azimuth, the electron emission was along the [110] direction. In all situations, the scattering plane coincided with the orbital plane of the storage ring, i.e., the horizontal plane. Photon energies between 800 and 860 eV were used to give Fe  $2p_{3/2}$  kinetic energies of 90–150 eV. Angular alignment was determined using LEED and laser reflection.

Typical Fe  $2p$  spectra for emission along the [110] direction [Fig. 1(a)] and [111] direction [Fig. 1(b)] are shown in Fig. 1. These spectra were collected with photon energy  $h\nu=835$  eV resulting in an electron kinetic energy of  $\sim 125$  eV at the Fe  $2p_{3/2}$  peak. It is important to note that the spectral differences discussed below were dependent only on the relative orientations of photon and minority electron spin and not on any absolute orientation for either quantity. In both sets of spectra the apparent spin-orbit splitting is reduced for the antiparallel orientation of photon and minority electron spin. This has been observed previously for these films<sup>16</sup> as well as for Fe(001) (Ref. 17) and is due to the magnetic exchange interaction which shifts the primarily majority-spin photoelectrons in the  $2p_{3/2}$  peak to higher binding energy

and the primarily minority-spin  $2p_{1/2}$  photoelectrons to lower binding energy. Venus *et al.*<sup>18</sup> also reported angular variations in the Fe  $2p$  dichroic asymmetry in angle-resolved photoemission, and attributed this to crystalline symmetry in the photoelectron state. These previous works focused on the *dichroic asymmetry* arising primarily from the magnetic exchange interaction. We are interested instead in isolating spin-dependent diffraction effects and therefore concentrate on the Fe  $2p$  *peak intensity* differences which depend only on the spin polarization of the photoelectrons. Along the [111] direction [Fig. 1(b)], our data demonstrate this spin-dependent intensity difference. It is observed primarily at the  $2p_{3/2}$  peak for the two electron- and photon-spin orientations. This is indicative of spin-dependent photoelectron diffraction along this direction. Much smaller intensity asymmetry is observed along the [110] direction [Fig. 1(a)]. No intensity asymmetry is observed for an unmagnetized film.

To focus on spin-dependent diffraction effects, it is necessary to separate exchange energy shift effects and intensity variations in the spin-orbit split  $2p$  doublet. To remove shifting effects, we individually align the cen-

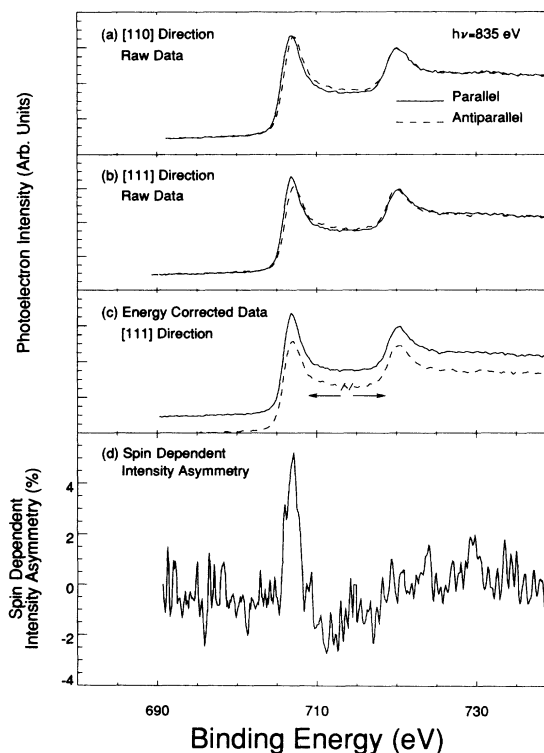


FIG. 1. Fe  $2p$  spectra for 4-ML Fe/Cu(001) along the [110] direction (a) and [111] direction (b) for parallel (solid curves) and antiparallel (dashed curves) photon and minority electron-spin orientation. The energy shifts are due to the magnetic exchange interaction of the spin-polarized photoelectrons. Note the intensity variations in the  $2p_{3/2}$  peak for the [111] direction and its absence along [110]. (c) A demonstration of how the peaks are shifted to remove exchange shift effects from the comparison of intensities. (d) Intensity asymmetry derived from the spectra in (b). The  $2p_{3/2}$  peak asymmetry is  $\sim 5\%$ . The data in the pre-peak region (binding energy  $< 705$  eV) was smoothed to reduce noise in the difference spectra in this region.

troids of both peaks. This is accomplished by shifting the  $2p_{3/2}$  peak for the antiparallel orientation to lower binding energy and the antiparallel  $2p_{1/2}$  peak to higher binding energy after separating the features in the region between the two peaks. This operation for the  $[111]$  direction is displayed in Figs. 1(b) and 1(c). Here, Fig. 1(b) is the raw data and Fig. 1(c) shows the energy shifts for the antiparallel data (the spectra are offset for clearer presentation). We note that the spectra are normalized to the low- and high-binding energy backgrounds to extract intensity differences in the  $2p$  photoemission peaks. Because each peak is spin polarized due to excitation by circularly polarized x rays, comparing the integrated intensities of peaks collected with parallel and antiparallel photon and electron-spin orientations isolates the spin-dependent diffraction effects.

To determine the intensity asymmetry in the data, we take the difference and divide by the sum of the two spectra on a channel by channel basis. We thereby obtain a spin-dependent intensity asymmetry (SIA) at each binding energy. This result is shown in Fig. 1(d) where the asymmetry varies from  $-2$  to  $5\%$ . This normalization scheme effectively equates the intensity of the  $2p_{1/2}$  features for the two spin orientations and places all the intensity asymmetry in the  $2p_{3/2}$  peak. The equalization of the  $2p_{1/2}$  features is due in part to the larger background and the Coster-Kronig broadening of this feature.<sup>19</sup> Along the  $[111]$  direction a peak asymmetry is consistently observed for the entire photon range examined. The peak asymmetries varied from  $\sim 2\%$  to as high as  $\sim 6\%$ . The observed intensity asymmetry is in marked contrast with the fairly isotropic intensity differences that are expected due to mixing of  $m_j$  states with  $2p_{3/2}$  and  $2p_{1/2}$  character.<sup>19</sup> The agreement between our experimental measurements and results of spin-dependent photoelectron diffraction calculations (which will be presented below for both angular and energy dependences of the intensity asymmetry) conclusively demonstrates that the observed intensity asymmetries derive primarily from spin-dependent diffraction.

The theoretical calculation of spin-polarized, multiple-scattering photoemission combines conventional photoemission and spin-polarized low-energy electron-diffraction methods.<sup>20</sup> For calculation of the excitation matrix element,  $\langle \Phi_E | H' | \Phi_E \rangle$ , the nonrelativistic approximation is incorporated and the dipole approximation for the interaction Hamiltonian is used. For this study, the Dirac matrix,  $\alpha$ , is replaced by Pauli matrices,  $\sigma$ . The selection rules for excitation by circularly polarized light restrict excitations to  $\Delta m_j = +1$  for right-circular polarization and  $\Delta m_j = -1$  for left-circular polarization. The Fe  $2p$  core-level is split into two sublevels due to the spin-orbit interaction, and transitions from the sublevels are governed by these selection rules.

After excitation, the internally polarized photoelectrons are multiply scattered inside the crystal in a way similar to spin-polarized LEED electrons. The single-site scattering matrix  $t_{kk'}^{\mu\mu'}$  is calculated using the Dirac equation<sup>21</sup> with spin-polarized potentials generated by a self-consistent linear augmented-plane wave band calculation.<sup>22</sup> This scattering matrix is converted to the ( $lms$ )

representation and used to construct layer diffraction matrices  $M_{gg}^{ss'}$ .

After that, the calculation proceeds as in a conventional photoemission calculation<sup>23</sup> except that the dimension of the layer diffraction matrices is doubled to include spin-dependent scattering and spin-flip effects.<sup>24</sup> Note that both spin-orbit coupling and exchange effects are accounted for since off-diagonal matrix elements are nonvanishing. In the calculation, the inner potential is set to 10 eV, and inelastic scattering is simulated by an imaginary potential of 4.5 eV. Since the electron kinetic energy is relatively low, only terms up to  $l=4$  are used for most calculations, but convergence is checked using terms up to  $l=6$  with insignificant differences found.

Because the calculated spin-dependent intensities are for an entire  $2p_{3/2}$  or  $2p_{1/2}$  manifold, the best comparison with experiment uses an integrated spin-dependent intensity asymmetry (or integrated SIA) defined as follows:

Integrated SIA( $h\nu$ )

$$= \frac{[I_{3/2}^+(h\nu)/I_{1/2}^+(h\nu) - I_{3/2}^-(h\nu)/I_{1/2}^-(h\nu)]}{[I_{3/2}^+(h\nu)/I_{1/2}^+(h\nu) + I_{3/2}^-(h\nu)/I_{1/2}^-(h\nu)]}, \quad (1)$$

where, for example,  $I_{3/2}^+$  is the parallel intensity integrated over the  $2p_{3/2}$  manifold. In Fig. 2, we show the calculated asymmetry (solid curve) along the  $[111]$  direction for a model with fcc Fe spacings ( $d_{12} = 1.8 \text{ \AA}$ ,  $d_{23} = 1.8 \text{ \AA}$ ) (Ref. 14) as a function of photon energy compared to the asymmetry extracted from the experimental data. In order to obtain an integrated SIA from our experimental data, the SIA curves [like that shown in Fig. 1(d)] are integrated over a 10-eV window centered at the  $2p_{3/2}$  peak. The integrated SIA gives a good agreement with the calculations and even reproduces the sign change in the asymmetry  $\sim h\nu = 840 \text{ eV}$ . Extending the integration limits will lower the asymmetry curve, but the choice of limits is not completely unrestricted due to the mixing of

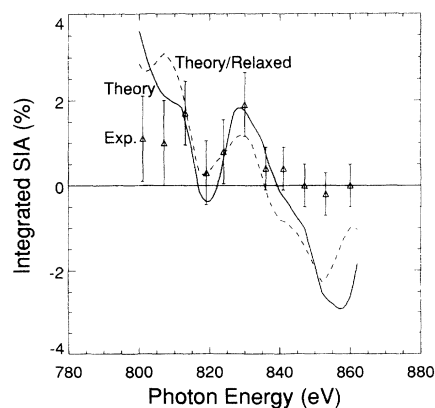


FIG. 2. Calculated (solid curve:  $d_{12} = d_{23} = 1.8 \text{ \AA}$ ,  $r_p = 0.19$ ; dashed curve:  $d_{12} = 1.9 \text{ \AA}$ ,  $d_{23} = 1.7 \text{ \AA}$ ,  $r_p = 0.17$ ) and measured intensity asymmetries along the  $[111]$  direction as a function of photon energy. The oscillatory behavior in the curves is due to spin-dependent photoelectron diffraction. Representative error bars are included with the experimental data, shown as discrete values (triangles). See text for details.

states with  $2p_{3/2}$  and  $2p_{1/2}$  character. However, the qualitative trends are all reproduced independent of the integration range and background parameters. The energy oscillations due to spin-dependent photoelectron diffraction are fundamental and are present even in the peak height intensities. Furthermore, variations of the structural parameters by  $\pm 0.2 \text{ \AA}$  destroys the agreement between the measurements and simulations. In fact, we have performed a detailed structural determination by varying the spatial parameters in the model and performing a quantitative  $r$  factor analysis of calculated and measured values. Our best fit occurs for  $d_{12} = 1.9 \text{ \AA}$  and  $d_{23} = 1.7 \text{ \AA}$  (dashed curve), with a Pendry  $r$  factor ( $r_p$ ) of 0.17, which is 9% better than the unrelaxed structure, a measurable difference. This is consistent with our previous determination<sup>14</sup> but exceeds those earlier results with a clear improvement in sensitivity to the small surface relaxations. Thus, the agreement between theory and experiment indicates that the intensity asymmetry arises from spin-dependent diffraction.

Next, we return to the angular dependences in the SIA. Figure 3(a) shows the results of calculations for scattering of 125-eV kinetic energy electrons (i.e.,  $h\nu = 835 \text{ eV}$ ) along the (110) azimuth as a function of electron polar emission angle from the sample normal. The arrow indicates the angle for the [111] direction studied experimentally. At this angle an integrated SIA of 1.02% is calculated. Note also that the calculated SIA displays sharp angular dependence along this azimuth. This is also evident in Fig. 3(b) where identical calculations for the (100) azimuth are presented. Here the SIA varies between  $-1.83$ – $3.26 \%$  as a function of electron emission angle and is 0.27% for emission along the [110] direction. This value is about four times lower than that for emission along the [111] direction and is again consistent with the qualitative trends in the experimental data. It is important to note that identical calculations omitting final-state diffraction events do not reproduce the energy and angular variations in the SIA. Additionally, because our measurements are made in mirror planes, other dichroic effects vanish.<sup>25</sup> (These effects also depend on the absolute photon helicity and not the relative spin orientations. Thus the internal cross check of varying both quantization axes is critical in isolating the SPPD effect.) Thus the agreement in both the angular and energy variations of the experimental and calculated intensity asymmetries demonstrates that the underlying cause of this intensity asymmetry is spin-dependent photoelectron diffraction.

Finally, in Fig. 3(c) we show the result of calculations which include both internal spin polarization and external spin detection for the Fe/Cu(001) system along the (110) azimuth. These are compared to the same calculations for no internal spin polarization (i.e., linearly polarized x rays) with external spin detection [Fig. 3(d)] and for internal spin polarization (circularly polarized x rays) with no external spin detection [the conditions of the current experiment, Fig. 3(a)]. With external spin detection [i.e., Figs. 3(c) and 3(d)], the integrated SIA is for the  $2p_{3/2}$  manifold only. Only with both internal spin polarization and external spin detection are asymmetries greater than a few percent predicted. Thus it appears

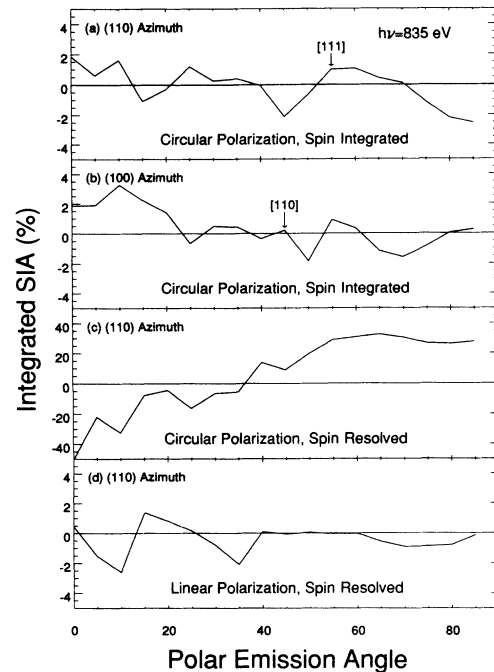


FIG. 3. Integrated SIA, calculated using Eq. (1) for scattering along (a) the (110) and (b) the (100) azimuths as a function of electron emission angle in degrees. Asymmetries of 1.02 and 0.27% for the [111] and [110] directions, respectively, are calculated. As throughout this work, circularly polarized x rays and a spin-integrating detector are used for (a) and (b). Integrated SIA calculated for the  $2p_{3/2}$  manifold only for (c) combined use of both circularly polarized x rays and external photoelectron spin detection and (d) linear polarization and external spin detection, along the (110) azimuth as a function of electron emission angle. Rapid angular variations are apparent for all combinations, but asymmetries as large as 10–50% are only observable using both circularly polarized x rays and external spin detection, i.e., (c).

that the combination of internally spin-polarized photoelectrons produced using circularly polarized radiation with external electron-spin detection provides the most powerful means of studying magnetic order.

In summary, we have measured spin-dependent photoelectron diffraction using circularly polarized x rays. The resultant spin-polarized  $2p$  photoemission peaks exhibit angle- and energy-dependent intensity variations due to spin-dependent final-state diffraction. The results are well described by spin-polarized photoemission, multiple-scattering calculations which also suggest that incorporating external photoelectron spin analysis will yield large effects and will be beneficial in future studies of magnetic materials.

Work performed under the auspices of the U.S. Department of Energy by the Lawrence Livermore National Laboratory under Contract No. W-7405-ENG-48. SSRL is supported by the Chemical Sciences Division of DOE/BES. The work at the University of Wisconsin–Milwaukee was supported by DOE DE-FG02-84ER45076.

- <sup>1</sup>S. S. R. Parkin, *Phys. Rev. Lett.* **71**, 1641 (1993).  
<sup>2</sup>B. P. Gurney *et al.*, *Phys. Rev. Lett.* **71**, 4023 (1993).  
<sup>3</sup>J. G. Tobin *et al.*, *Phys. Rev. Lett.* **70**, 4150 (1993).  
<sup>4</sup>J. G. Tobin *et al.*, *Phys. Rev. Lett.* **68**, 3642 (1992).  
<sup>5</sup>S. A. Chambers *et al.*, *Phys. Rev. B* **36**, 8992 (1987).  
<sup>6</sup>D. A. Steigerwald and W. F. Egelhoff, *Phys. Rev. Lett.* **60**, 2558 (1988).  
<sup>7</sup>D. Pescia *et al.*, *Phys. Rev. Lett.* **60**, 2559 (1988).  
<sup>8</sup>D. P. Pappas *et al.*, *Phys. Rev. Lett.* **64**, 3179 (1990).  
<sup>9</sup>C. Liu *et al.*, *Phys. Rev. Lett.* **60**, 2422 (1988).  
<sup>10</sup>D. D. Chambliss *et al.*, *J. Vac. Sci. Technol. A* **10**, 1993 (1993);  
D. D. Chambliss *et al.*, in *Magnetic Ultrathin Films: Multilayers and Surfaces/Interfaces and Characterization*, edited by B. T. Jonker *et al.*, MRS Symposia Proceedings No. 313 (Materials Research Society, Pittsburgh, 1993), p. 713.  
<sup>11</sup>G. Schütz *et al.*, *Phys. Rev. Lett.* **62**, 2620 (1989).  
<sup>12</sup>B. Sinkovic and C. S. Fadley, *Phys. Rev. B* **31**, 4665 (1985); B. Sinkovic *et al.*, *Phys. Rev. Lett.* **55**, 1227 (1985); B. Hermsmeier *et al.*, *ibid.* **62**, 478 (1989); E. Zhang *et al.*, *Bulletin APS* **39**, 904 (1994).  
<sup>13</sup>M. T. Johnson *et al.*, *J. Phys. C* **20**, 4385 (1987).  
<sup>14</sup>J. G. Tobin *et al.*, in *Advances in Surface and Thin Film Diffraction*, edited by T. C. Huang *et al.*, MRS Symposia Proceedings No. 208 (Materials Research Society, Pittsburgh, 1991), p. 283.  
<sup>15</sup>K. G. Tersell and V. P. Karpenko, *Nucl. Instrum. Methods Phys. Res. Sec. A* **291**, 511 (1990); L. J. Terminello *et al.*, *ibid.* **319**, 271 (1992).  
<sup>16</sup>G. D. Waddill *et al.*, *Phys. Rev. B* **46**, 552 (1992).  
<sup>17</sup>L. Baumgarten *et al.*, *Phys. Rev. Lett.* **65**, 492 (1990).  
<sup>18</sup>D. Venus *et al.*, *J. Phys.* **5**, 1239 (1993).  
<sup>19</sup>H. Ebert *et al.*, *Phys. Rev. B* **44**, 4406 (1991).  
<sup>20</sup>R. Feder, in *Polarized Electrons in Surface Physics*, edited by R. Feder (World Scientific, Singapore, 1985).  
<sup>21</sup>R. Feder *et al.*, *Z. Phys. B* **52**, 31 (1983).  
<sup>22</sup>H. J. Jansen and A. J. Freeman, *Phys. Rev. B* **30**, 561 (1984).  
<sup>23</sup>C. H. Li *et al.*, *Phys. Rev. B* **17**, 3128 (1978).  
<sup>24</sup>A. Ormeci *et al.*, *Phys. Rev. B* **41**, 4524 (1990).  
<sup>25</sup>H. P. Oepen *et al.*, *Phys. Rev. Lett.* **56**, 496 (1986).